Published in final edited form as:
J Immunol. 2009 July 15; 183(2): 1375–1383. doi:10.4049/jimmunol.0901005.

Treatment with a C5aR Antagonist Decreases Pathology and Enhances Behavioral Performance in Murine Models of Alzheimer's Disease[1]

Maria I. Fonseca[*], **Rahasson R. Ager**[*], **Shu-Hui Chu**[*], **Ozkan Yazan**[*], **Sam D. Sanderson**[†], **Frank M. LaFerla**[‡], **Stephen M. Taylor**[§], **Trent M. Woodruff**[§], and **Andrea J. Tenner**[2,*,‡,¶]

[*]Department of Molecular Biology and Biochemistry, University of California, Irvine, CA 92697

[†]School of Allied Health Professions, University of Nebraska, Omaha, NE 68198

[‡]Department of Neurobiology and Behavior and Institute for Brain Aging and Dementia, University of California, Irvine, CA 92697

[§]School of Biomedical Sciences, University of Queensland, St. Lucia, Queensland, Australia

[¶]Department of Pathology and Laboratory Medicine, University of California, Irvine, CA 92697

Abstract

Alzheimer's disease (AD) is an age-related dementia, characterized by amyloid plaques, neurofibrillary tangles, neuroinflammation, and neuronal loss in the brain. Components of the complement system, known to produce a local inflammatory reaction, are associated with the plaques and tangles in AD brain, and thus a role for complement-mediated inflammation in the acceleration or progression of disease has been proposed. A complement activation product, C5a, is known to recruit and activate microglia and astrocytes in vitro by activation of a G protein-coupled cell-surface C5aR. Here, oral delivery of a cyclic hexapeptide C5a receptor antagonist (PMX205) for 2–3 mo resulted in substantial reduction of pathological markers such as fibrillar amyloid deposits (49 – 62%) and activated glia (42– 68%) in two mouse models of AD. The reduction in pathology was correlated with improvements in a passive avoidance behavioral task in Tg2576 mice. In 3xTg mice, PMX205 also significantly reduced hyperphosphorylated tau (69%). These data provide the first evidence that inhibition of a proinflammatory receptor-mediated function of the complement cascade (i.e., C5aR) can interfere with neuroinflammation and neurodegeneration in AD rodent models, suggesting a novel therapeutic target for reducing pathology and improving cognitive function in human AD patients.

[1]This research was supported by National Institutes of Health Grants NS 35144 (to A.J.T.) and P50 AG-00538, National Institutes of Health Training Grant NS-007444 (to R.R.A.), and a Project Grant from the National Health and Medical Research Council of Australia (Grant 455856 to S.M.T.).

[2]Address correspondence and reprint requests to Dr. Andrea J. Tenner, Department of Molecular Biology and Biochemistry, University of California, Irvine, 3205 McGaugh Hall, Irvine, CA 92697. atenner@uci.edu.

Disclosures

The authors have no financial conflicts of interest.

Alzheimer's disease (AD),[3] the most common age-related neurodegenerative disorder associated with progressive loss of cognitive function, displays characteristic neuropathological changes, including synaptic and neuronal loss (1), neurofibrillary tangles (NFTs) (2), extracellular senile plaques composed of amyloid (Aβ) protein deposits (3), and inflammatory glia (4, 5). In human studies, clinically significant cognitive decline occurs at the stage of the disease in which fibrillar Aβ plaques and NFTs are present; however, it is becoming increasingly evident that the presence of fibrillar plaques is not sufficient for clinical diagnosis of AD (6), and thus other factors are critical in loss of cognition. Studies in both AD patients and transgenic mouse models of AD suggest that it is likely that multiple, overlapping processes contribute to neuronal degeneration and cognitive loss.

The complement system is a well-known powerful effector mechanism of the immune system, providing protection from infection and resolution of injury (7). Complement activation generates activation fragments that include C3a and C5a, which interact with cellular receptors to recruit and/or activate phagocytes (including microglia and astrocytes) (8). Activated microglia can be phagocytic, but they also can secrete several proinflammatory cytokines, as well as reactive oxygen species and NO, which if not regulated can create a neurotoxic inflammatory environment that can accelerate pathology and neuronal dysfunction (9). Extensive studies have shown fibrillar (β-sheet containing) Aβ activates both the classical and alternative complement pathways (10, 11) and that complement factors are prominently associated with Aβ plaques containing the fibrillar Aβ peptide (12, 13) rather than with diffuse amyloid plaques (lacking β-sheet), even early in the disease, as fibrillar plaques appear (14, 15), as well as on some NFTs (16). Since reactive microglia are rapidly recruited to newly formed fibrillar plaques in mouse models (17), it can be hypothesized that fibrillar amyloid deposits initiate events such as complement activation and subsequent glial recruitment that, if not sufficiently regulated, could accelerate neuropathology and disturb neuronal function (18).

Mouse models of AD and/or neurodegeneration show similar association of the complement components C1q, C3, and C4 (19 –21) with fibrillar amyloid plaques. Interestingly, in rodent models evidence of both detrimental and neuroprotective consequences of complement activation have been reported (19, 22, 23), and C1q and C3 have also been shown to contribute to synaptic pruning during normal development (24). The use of inhibitors of specific downstream complement cascade events, such as recruitment and activation of inflammatory glia, would avoid inhibiting the potentially beneficial consequences of complement activation. C5a receptor antagonists have been shown to be beneficial in rodent models of acute inflammation (25–28). The present study was conducted to ascertain the involvement of the potent inflammatory complement factor C5a in AD and to assess a potential therapeutic approach. Data presented herein demonstrate that treatment with the small-molecular mass cyclic hexapeptide C5a receptor antagonist PMX205 significantly reduces neuropathology and improves performance in a passive avoidance task

[3]Abbreviations used in this paper: AD, Alzheimer's disease; Aβ, β-amyloid peptide; APP, amyloid precursor protein; DIEA, *N*,*N*-diisopropylethylamine; GFAP, glial fibrillary acidic protein; NFT, neurofibrillary tangle; PMX205, cyclic hexapeptide hydrocinnamate-(L-ornithine-proline-D-cyclohexylalanine-tryptophan-arginine; Py-BOP, benzotriazol-1-yloxytris(dimethylamino)phosphonium hexafluorophosphate; SYN, synaptophysin; UT, untreated.

for contextual memory in mouse models of AD. Thus, inhibition of complement-induced inflammation might dramatically slow the “snowballing” cascade of cognitive decline in AD, even after the initial stages of impairment are diagnosed.

Materials and Methods

Mice

Two transgenic mouse models were used. Tg2576 from K. Hsiao (29), expressing human amyloid precursor protein (APP)695 containing the double mutation KM670/671NL (Swedish mutation), inserted into hamster prion protein on C57BL/6 genetic background were maintained by back-crossing to B6/SJL (The Jackson Laboratory). Nontransgenic (B6/SJL) littermate mice were used as controls. Also used were 3xTg mice harboring the APP Swedish mutation, a human four-repeat (tau P301L) mutation and a knock-in mutation of presenilin 1 (PS1M146V) (30). All genotypes were confirmed by PCR and/or quantitative PCR (3xTg). All animal experimental procedures performed were reviewed and approved by the University of California at Irvine Institutional Animal Care and Use Committee.

Synthesis of the C5a receptor antagonist PMX205

PMX205 was synthesized via a modification of the methods previously described (31) by generating the linear hexapeptide via solid-phase synthesis rather than solution-phase synthesis. The cyclic hexapeptide hydro-cinnamate-(L-ornithine-proline-D-cyclohexylalanine-tryptophan-arginine) (PMX205) was synthesized by standard solid-phase methods on a preloaded Arg-Wang resin using the Fmoc (9-fluorenylmethoxycarbonyl) scheme of orthogonal residue coupling and deprotection. The linear hexapeptide was obtained by cleavage in trifluoroacetic acid with appropriate scavengers, precipitation in cold ether, and HPLC purification on C18 analytical and preparative columns. PMX205 was obtained by intramolecular cyclization of the linear hexapeptide as follows: the linear hexapeptide was dissolved in dimethylformamide plus 1 equivalent of *N*,*N*-diisopropylethylamine (DIEA) and cooled to −10°C. A second solution of 1.1 equivalents of benzotriazol-1-yloxytris(dimethylamino)phosphonium hexafluorophosphate (PyBOP) and 1 equivalent of DIEA was dissolved in dimethylformamide and cooled to −10°C. The peptide solution was added dropwise to the PyBOP solution with stirring over a 15-min period and the reaction mixture was stirred at −10°C for 5 h. Additional DIEA was added as needed to maintain the pH between 7.5 and 8.0. PMX205 was obtained by adding the reaction solution dropwise to an excess of cold ether to precipitate the PMX205. The drug was purified by HPLC, and the molecular mass (841) was verified by MALDI mass spectrometry (MS 841 MH^+).

Aβ assembly assays

Preparation and assay of fibrillar Aβ was done as previously described (32). Briefly, to prepare fibrillar Aβ_{42}, 2 mM Aβ_{42} (C. Glabe, University of California, Irvine (32)) in 100 mM NaOH was sonicated briefly (30 s). Samples were subsequently diluted to 45 μM in fibrillization buffer (100 mM NaCl, 10 mM HEPES (pH 7.4), containing 0.02% sodium azide) and stirred at room temperature in the presence and absence of 0 –300 μM PMX205. For kinetic assessment of fibril formation, mixtures were assayed each day for 6 consecutive

days of coincubation. Ten microliters of the Aβ_{42} mixtures was combined with 120 μl of 3 μM thioflavine T in fibrillization buffer, and the fluorescence emission at 482 nm, indicative of the degree of fibrillization, was measured alone using a Gemini XPS plate reader (Molecular Devices).

Animal treatment with PMX205

Tg2576 mice were treated (starting at or after the initiation of plaque pathology) for 2–3 mo with the C5aR antagonist PMX205 given in the drinking water only (10 –20 μg/ml, equivalent to ~3– 6 mg/kg/day) or both in drinking water (10 –20μ/ml) and s.c. (1 mg/kg) twice weekly throughout the treatment period. Untreated transgenic animals of same age were used as controls. Nontransgenic littermates were similarly treated or not treated with the drug. 3xTg mice were also treated with PMX205 in the drinking water. Due to the low pathology of the males, similar to that previously reported (33), only female mice of this strain were used for these studies.

Immunohistochemistry and image analysis

Mice were anesthetized with a mixture of ketamine/xylazine (67/27 mg/kg) and perfused with PBS. After dissection, half of the brain was immediately frozen on dry ice and the other half was fixed overnight with 4% paraformaldehyde (for immunohistochemistry). Thereafter, fixed tissue was stored in PBS/0.02% Na azide at 4°C until use. Immunohistochemical procedures were done as previously described on coronal, 40-μm vibratome sections (19). Briefly, after pretreating with 50% formic acid (only for amyloid staining), and blocking endoperoxidase with 3% H_2O_2/10% MeOH in TBS and nonspecific binding with 2% BSA/0.1% Triton X-100/TBS, sections were incubated with the corresponding primary Abs or control IgG. Primary Abs were detected with biotinylated secondary Abs against the corresponding species, ABC complex, and diaminobenzidine (Vector Laboratories), following the manufacturer's instructions. For fluorescent labeling, Cy3-streptavidin (Jackson ImmunoResearch Laboratories; 1/200) was used after the biotinylated secondary Ab.

Abs used were: mouse monoclonal 6E10 Abs (1 μg/ml) (Senetek) for total amyloid, and rabbit polyclonal glial fibrillary acidic protein (GFAP) (4 μg/ml) (Dako) and rat monoclonal anti-CD45 (1 μg/ml) and anti-CD68 (5 μg/ml) Abs (Serotec) for astrocytes and microglia, respectively. Presynaptic terminals were labeled with rabbit polyclonal anti-synaptophysin (SYN; 3 μg/ml) (Dako). Hyperphosphorylated tau was labeled using mouse mAb AT100 (recognizing phosphorylated Ser^{212} and Thr^{214} tau) (0.02 μg/ml) (Pierce). Fibrillar Aβ was stained with 1% thioflavine as previously described (19).

Immunostaining was observed under a Zeiss Axiovert-200 inverted microscope. Images were acquired with a Zeiss Axiocam high-resolution digital color camera (1300 × 1030 pixels) using Axiovision 4.1 or 4.6 software and analyzed using the same software (Zeiss). For SYN staining, images were taken using a Zeiss LSM 510 Meta laser scanning confocal microscope and analyzed using KS300 software (Zeiss). Immunostaining for each marker was done simultaneously in coronal sections at similar distance from bregma in all animals compared. Digital images were obtained using the same settings, and the segmentation

parameters were constant per given marker and experiment. Similar areas were evaluated in all the animals compared per marker. Total (Aβ) and fibrillar (thioflavine) plaque area as well as glia area (CD45, CD68, GFAP) surrounding the plaque (identified by colocalization with thioflavine) was quantified in cortex and hippocampus in the Tg2576 or in subiculum area in the 3xTg model. SYN was quantified in the CA3 (CA3a and CA3c) field of hippocampus. Percentage of immunopositive area (immunopositive area/total image area × 100) was determined for all the markers studied by averaging several images per section that cover the region of study. The mean value for each animal results from the analysis of two to four sections. The average of the means per group is presented. All of the markers were studied in several untreated and treated animals from at least two different trials. Single ANOVA statistical analysis was used to assess the differences in plaque area, glial reactivity, and neuronal integrity among the animal groups (treated and untreated).

Behavioral assays

Male and female mice were tested using a passive step-through inhibitory avoidance test (34). The apparatus (San Diego Instruments) consists of two chambers, each 21 × 25.5 × 16.5 cm, separated by a sliding door. During training, mice were placed in the starting chamber for a period of 30 s, after which the chamber was illuminated and the sliding door opened. Upon the mice completely entering the dark chamber, with all four paws touching the chamber floor, the mice received a mild 0.26- to 0.27-mAmp shock for a period of 1 s. After receiving the shock, the mice were left in the dark chamber for an additional 4 s before being removed and returned to their holding cage. Retention was then tested 24 h later by placing the mice in the lighted chamber with open door access to the dark chamber. Latency to enter the chamber was recorded, using a maximum of 180 s latency before terminating the trial.

As a measure of spontaneous alternation and activity, mice were tested using a metallic Y-maze apparatus. The Y-maze consists of arms measuring 23 × 6 × 16 cm with a plastic cover to reduce light but still allow the experimenter to score the trial. A mouse was given one trial of exploratory time, which consisted of a 5-min interval. During the trial, the total number of alternations and arm entries was recorded. The percentage alternation and total number of arm entries were recorded and expressed as previously described (35). Statistical analyses were done using a Kruskal-Wallis ANOVA test, as some groups displayed a nonparametric distribution, followed by a Mann-Whitney *U* test.

ELISA assays for soluble and insoluble $A\beta_{40}$ and $A\beta_{42}$ amyloid

Briefly, frozen half cortical or hippocampal sections were pulverized on dry ice and homogenized in 5× vol (5 μl/mg cortical tissue) or 10× vol (10 μl/mg hippocampal tissue) of T-PER reagent (Pierce) with protease inhibitor cocktail (Roche Diagnostics, catalog no. 118836153001). The homogenates were sonicated (1-s pulse) and centrifuged at 100,000 × *g* at 4°C for 1 h, and the resulting supernatant was collected as the T-PER/detergent-soluble fraction. The pellet was then resuspended to the starting volume in 70% formic acid. After centrifugation at 100,000 × *g*, 4°C for 1 h, the supernatant was collected and stored at −80°C as the T-PER-insoluble fraction. Immulon 2HB flat-bottom wells (Thermo Scientific) were first coated with monoclonal anti-Aβ1-16 Ab (from Dr. W. van Nostrand, Stony Brook

University, New York, NY) at 33 μg/ml in 0.1 M carbonate buffer at pH 9.6 overnight at 4°C. Wells were subsequently blocked with 3% BSA in PBS at 37°C for 3 h. After plates were washed, appropriately diluted samples or human ultrapure Aβ_{40} or Aβ_{42} standards (Millipore) were loaded into wells in triplicate and allowed to incubate overnight at 4°C in capture buffer (pH 7.0) (20 mM sodium phosphate, 0.4 M NaCl, 2 mM EDTA, 0.3% BSA, 0.05% CHAPS, and 0.05% Na azide). Plates were washed and then probed with either biotinylated monoclonal anti-Aβ_{40} Ab (C49) or anti-Aβ_{42} (D32) Ab (from Dr. V. Vasilevko, University of California, Irvine, CA) in detection buffer (pH 7.0) (20 mM sodium phosphate, 0.4 M NaCl, 2 mM EDTA, 1% BSA, and 0.02% thimerosal) overnight at 4°C. Streptavidin-HRP (1/4000; Pierce) in detection buffer was added and incubated at 37°C for 3 h. Plates were developed with the addition of Ultra TMB-ELISA substrate (Pierce) followed by 0.8 M O-phosphoric acid to stop the reaction. Plates were subsequently read at 450 nm using a SpectraMax Plus plate reader (Molecular Devices).

Results

The C5a receptor antagonist PMX205 is a nontoxic cyclic hexapeptide that reduces pathology in transgenic mouse models of AD

PMX205 was previously shown to reduce acute inflammation in rodent models of injury in which complement activation occurs (25, 26). Initial trials were performed to assess toxicity of the drug in wild-type and AD transgenic mice when chronically administered s.c. or in the drinking water. There was no weight loss or change in daily water intake in wild-type mice, Tg2576 or 3xTg, when treated for 12 wk with PMX205 in any dose or delivery mode (data not shown). However, all preliminary experiments demonstrated decreased amyloid deposits and glial reactivity in the brain of the transgenic mouse models whether the drug was delivered in the drinking water alone (at 10 or 20 μg/ml) for 8 –12 wk, or if provided both in the drinking water (10 or 20 μg/ml) plus a s.c. injection (1 mg/kg body weight) twice a week (Table I). Larger statistically significant decreases in pathology were detected when a higher dose of the drug was delivered to the animals in the drinking water (Table I). Based on these preliminary results, the 20 μg/ml dose was chosen for all subsequent therapeutic studies.

To determine whether PMX205 had a direct influence on Aβ assembly, freshly dissolved amyloid (45 μM) was incubated with 0 –300 μM PMX205 for 6 days under conditions in which fibrils are generated and the amount of fibrils formed was assessed. The rate of fibril formation, using thioflavine reactivity as a measure of β-sheet fibril accumulation, was unaffected by the presence of PMX205 at pharmacologically relevant concentrations of the drug in vivo (data not shown). At very high concentrations of PMX205, 100 and 300 μM (84 and 252 μg/ml, respectively), Aβ_{42} fibril assembly was inhibited. However, since it has been shown that oral dosing of PMX205 results in maximal plasma levels of <1 μg/ml (25), there is no evidence that the effect of PMX205 in vivo is due to interactions of the drug with Aβ itself.

PMX205 treatment decreases both total amyloid deposits and fibrillar amyloid plaques in Tg2576 mice

Tg2576 mice were treated with PMX205 at 20 μg/ml in the drinking water ($n = 17$) from 12 to 15 mo of age, the time frame at which there is a rapid accumulation of amyloid deposits in these animals. Untreated Tg2576 animals ($n = 11$) were used as controls. After 3 mo, animals treated with PMX205 showed significantly less fibrillar plaque load (thioflavine reactivity) than did untreated animals (Fig. 1, *A* and *B*). Image analysis of cortex and hippocampal areas demonstrated a 44% decrease in thioflavine labeling in treated animals compared with untreated animals (Fig. 1*E*). While there was expected variability in the degree of pathology among animals, the difference between the treated and untreated animals was highly statistically significant ($p < 0.0006$). Immunostaining with monoclonal 6E10 Ab, which recognizes diffuse as well as fibrillar human amyloid deposits, showed a similar, albeit of less magnitude, decrease in total amyloid load (29%, $p < 0.03$) (Fig. 1, *C*, *D*, and *F*).

PMX205 treatment results in less reactive glia surrounding fibrillar amyloid plaques

C5a receptors are expressed on microglia and astrocytes (8), and in vitro they have been shown to mediate chemotaxis in response to the activation peptide (36). Treatment with the C5aR antagonist PMX205 reduced the level of plaque-associated activated microglia detected with anti-CD45 by 49% ($p < 0.02$) in the treated Tg2576 mice compared with untreated Tg2576 animals (Fig. 2, *A*–*C*). The decrease in CD45 reactivity was positively correlated with the decrease in thioflavine area ($R = 0.82$, $p < 0.0001$) (Fig. 2*D*). Similarly, CD68 (macrosialin, a marker for phagocytic microglia) was also decreased (53%, $p < 0.01$) in the PMX205-treated animals (data not shown) compared with drug-free controls.

Astrocytes in the vicinity of the thioflavine-positive plaques (Fig. 2, *E* and *F*) were also decreased (54%, $p < 0.003$) in PMX205-treated Tg2576 animals compared with untreated Tg2576 as measured by GFAP immunoreactivity (Fig. 2*G*). Image analysis of colocalization of GFAP/thioflavine showed that the ratios of GFAP/thioflavine were similar in both treated and untreated groups. The decrease in GFAP correlated with thioflavine reduction ($R = 0.74$, $p < 0.0.01$) (Fig. 2*H*).

PMX205 treatment causes significant decreases in hyperphosphorylated tau as well as fibrillar plaques in the 3xTg mouse model

To study the effect of PMX205 in an AD mouse model that shows tau pathology as well as plaque pathology, the 3xTg mouse model generated and characterized by LaFerla and coworkers (30) was used. 3xTg animals were treated from 17 to 20 mo (at which time these mice begin to accumulate fibrillar amyloid) with the same dose of PMX205 in the drinking water as used with the Tg2576 mice. Two different trials were performed with similar results, and thus the average of the data from both trials is presented here. Hyperphosphorylated tau was strikingly reduced in the treated animals (69%, $p < 0.02$) as demonstrated by image analysis (Fig. 3, *A*–*C*). A significant reduction in thioflavine area was also seen (49%, $p < 0.05$) (Fig. 3*D*) and was accompanied by a trend of a decrease in CD45 staining (45%, $p < 0.12$) (Fig. 3*E*).

Treatment with the C5a receptor antagonist increases SYN in the hippocampus of Tg2576 mice

In the 3xTg model, treatment with PMX205 decreased hyperphosphorylated tau reactivity, which is indicative of a reduction in neurodegeneration. To establish if the antagonist would also improve neuronal integrity in the Tg2576 model, the effect on the presynaptic marker SYN was assessed. SYN labeling was examined in the stratum lucidum of the CA3 field of hippocampus area, which is rich in SYN-positive presynaptic terminals. Confocal imaging (Fig. 4, *A* and *B*) and quantification of the SYN immunolabeled area showed a significant increase of 33% ($p < 0.03$) (Fig. 4*C*) in the treated Tg2576 mice compared with the untreated animals. A similar increase (27%, $p < 0.05$) was observed after quantification of images obtained by conventional fluorescent microscopy in a larger sample of animals (untreated (UT) = 10, PMX205 = 12).

T-PER-insoluble amyloid levels are reduced in PMX205-treated animals

In accordance with the reduced thioflavine-positive fibrillar plaque load observed in PMX205-treated mice, we observed reductions in cortical amyloid levels as assayed via Aβ ELISA. Formic acid-soluble (T-PER-insoluble) amyloid levels were lower in treated Tg2576 mice ($n = 10$) when compared with untreated Tg2576 control animals ($n = 6$) (Fig. 5, *A* and *B*). Aβ_{40} levels were reduced by 21%, while Aβ_{42} levels were reduced by 43%. While substantial mean reductions were seen, the differences did not reach statistical significance ($p = 0.198$ and $p = 0.272$), likely due to interanimal variability. In contrast, T-PER-soluble Aβ_{40} was slightly elevated in treated animals, while there was no observed difference in soluble Aβ_{42} levels between treated and untreated mice (Fig. 5, *C* and *D*).

PMX205 treatment rescues Tg2576 cognitive impairment in passive avoidance task

To determine whether the significant reduction in both plaque deposits and reactive glia observed after treatment with PMX205 led to improved cognitive function, we evaluated working memory utilizing the Y-maze spontaneous alternations task in Tg2576 mice at 15 mo of age. While we observed the reported hyperactivity associated with the Tg2576 mouse, as these animals had higher average total arm entries than those of nontransgenic mice (data not shown), there were no memory impairments found in Tg2576 mice vs nontransgenic littermate control mice in this task and no effects of PMX205 treatment were observed (data not shown).

To assess contextual memory impairments, a step-through passive avoidance task was employed. Tg2576 mice showed a significant reduction in memory retention when compared with non-transgenic PMX205 untreated controls. Fifteen-month-old Tg2576 mice delayed entry into the dark chamber for only 67.1 s ($n = 8$) vs 134.s ($n = 14$) for nontransgenic littermate mice at 24 h ($p < 0.04$, Fig. 6*A*). Importantly, the reduction in Tg2576 mice memory retention was rescued after PMX205 treatment for 12 wk, as time to enter the dark chamber at 24 h was 130.4 s for these animals ($n = 5$). Further analysis on hippocampal extracts from PMX205-treated mice revealed a negative correlation between animal performance and detergent-insoluble Aβ_{40} and Aβ_{42} levels ($R = -0.87$, $p = 0.058$ and $R = -0.96$, $p < 0.01$, respectively) (Fig. 6, *B* and *C*). Correlation analysis of detergent-

soluble Aβ_{40} and Aβ_{42} and cognitive performance of the PMX205-treated mice show similar results (analysis not shown).

Discussion

The complement system has been implicated in the pathology of AD, but to date no one has examined the specific role of C5a or C5aR in this disease. Our data clearly demonstrate that treatment with the C5a receptor antagonist PMX205 results in significant and substantial (up to 69%) decreases in pathology in two different mouse models of AD and improved performance in a passive avoidance task for contextual memory. A distinct advantage of this small hexapeptide is that the point of inhibition is downstream of complement activation, avoiding interference with upstream potentially protective complement activation events.

Fibrillar amyloid activates the complement cascade both in vitro and in vivo (reviewed in Ref. 37). Complement factors and reactive microglia and astrocytes are found associated with Aβ plaques containing the β-sheet fibrillar Aβ peptide rather than diffuse amyloid plaques (12, 38). Since activation of the complement cascade results in the production of complement activation products C5a and C3a that are chemotactic for microglia and astrocytes (39), it was hypothesized that at least part of the recruitment of these cells to the plaque area was due to C5a, the more robust and potent chemotactic peptide of the two anaphylatoxins (reviewed in Ref. 8). These recruited cells can be phagocytic, but can also be “activated” to different functional states depending on the sum of the stimulatory signals they encounter, secreting proinflammatory cytokines, reactive oxygen species, and NO. This elevated inflammatory reaction in the area of the plaque could ultimately accelerate the neuronal dysfunction and cognitive decline seen in the human disease (40, 41).

C5a-C5aR signaling has been shown to synergize with other receptor signaling, including P2Y6 (42) and TLR in multiple tissues including the brain (43– 45). Aβ has been reported to engage TLR2 and TLR4 (46, 47), and thus inflammation in response to Aβ interactions with receptors on C5a-recruited glia cells may be significantly enhanced relative to the response of microglia in the absence of C5a. This enhanced inflammation would accelerate neurotoxicity and/or neuronal dysfunction, while inhibition of the C5a-C5aR interaction would reduce gliosis and inflammation and subsequently the amyloid deposition and neuronal dysfunction as seen here. While further studies are needed to more precisely assess the different amyloid assembly states in the PMX205-treated animals, the substantial and significant reduction in fibrillar plaques in conjunction with reduced glia is consistent with results of others in which reduction of inflammation reduces amyloid load (48). Recently it was reported that DBA/2 mice (which are C5-deficient) carrying the human APP transgene show significantly less accumulation of amyloid peptide than did the C5-sufficient C57BL/6 mouse with the identical transgene (49). Additionally, whole-genome quantitative trait linkage mapping identified an association of this difference in amyloid accumulation with the C5 gene mutation, suggesting a detrimental role for C5 or the downstream complement activation products in this neuropathology, consistent with the reduced plaque accumulation as a result of C5aR antagonist treatment seen in this study (Fig. 1). No direct effect of the drug on amyloid fibrillization was seen in our in vitro studies.

It has been reported that the introduction of a proinflammatory environment within the CNS of aged mice can lead to impaired contextual memory as assayed in the passive avoidance task, and that inhibition of such proinflammatory events can lead to improved performance in the task (50). In the examination of behavior of our mice, consistent with earlier publications, we observed the characteristic hyperactivity associated with Tg2576 mice. However, in the present study, Tg2576 mice at 15 mo of age displayed comparable arm alternation percentages during the Y-maze testing to those of no-transgenic controls. The difference between our studies and previous reports (35, 51) could be due to either the difference in the age of the mice used in these studies or the difference in the genetic background of the mice, as our founder males were bred against B6/SJL mice vs C57BL/6. Thus, amyloid deposition and glial activation do not affect working memory in our colony of Tg2576 animals at this age as assayed in the spontaneous alternation Y-maze task, nor is C5a-mediated inflammation involved in the hyperactivity associated with Tg2576 mice. In contrast, a significant impairment in contextual memory in our 15-mo-old Tg2576 untreated mice was observed when compared with untreated nontransgenic controls of the same age. Additionally, after a 12-wk treatment with PMX205, the Tg2576 mice displayed improved performance vs untreated Tg2576 mice in the task, which approached statistical significance ($p = 0.1$; likely due to the limited number of treated animals assayed for contextual memory performance). Memories dependent on specific environmental context are highly dependent on the hippocampus. Subsequent analysis showed a strong correlation between hippocampal-insoluble amyloid loads and memory performance in PMX205-treated mice (Fig. 6, *B* and *C*). The data support the hypothesis that inhibition of complement-mediated inflammation, through C5aR/CD88 blockade, can result in improved memory performance in Tg2576 mice. To our knowledge, this is the first time inhibition of CD88 has been linked to improved cognitive performance.

In support of the hypothesized role of complement in AD, in vivo studies in which the C1q gene (which is required for the classical complement activation pathway) was knocked out in the Tg2576 mouse model of AD demonstrated a 50% reduction in microgliosis and astrocytic activation accompanied by a >60% rescue of neuronal integrity (MAP2 and SYN) (19) relative to the complement-sufficient Tg2576 mice. While this and other studies (52) have suggested detrimental effects of complement activation in the AD brain, additional investigations have suggested that at least some of the complement factors can decrease the neuropathology in some mouse models of AD (22, 53) or limit the detrimental responses to neurodegenerative stimuli in other injury models (23, 54 –56). One explanation for the reported accelerated pathology in C3-deficient (22) or C3-inhibited (53) AD mouse models is that the lack of recruited microglia and/or lack of C3b as an opsonin to enhance phagocytosis slowed Aβ clearance and ultimately resulted in an increase in degenerating neurons. C3 deposition, presumably via the alternative pathway, was seen in the Tg2576 $C1q^{-/-}$ mouse (21) and thus could provide the C3b opsonic benefit in these mice that would not be functional in the $C3^{-/-}$ or Crry overexpressing model. Note that a beneficial role for C3a via stimulation of nerve growth factor production or other neuroprotective function (55, 57, 58) has not yet been investigated in this model. Similarly, in the model reported herein in which the C5aR antagonist blocks C5a access to CD88, presumably limiting glial activation,

the beneficial roles of upstream complement components, such as C3 and C1q (22, 23, 53), remain available.

One question that remains unclear, however, is that if the alternative pathway was being activated in the Tg2576 C1q$^{-/-}$ mice, as evidenced by C3b deposition on plaques (21), why did the alternative complement pathway generation of C5a in the Tg2576 C1q$^{-/-}$ mice (19) not result in the same level of glial recruitment and detrimental activation as in the C1q-(classical complement pathway) sufficient Tg2576 mice. There are several factors that could contribute to this difference. First, the classical pathway of complement activation generates molecularly distinct C3- and C5-cleaving enzymes (C3 and C5 convertases), C4bC2b and C4bC2bC3b, respectively, from those of the alternative pathway, C3bBb and C3bBbC3b, respectively (37), and it is currently unknown whether and to what extent these C3 and C5 convertases have different kinetic properties and/or different susceptibility to regulatory components, all of which would contribute to the relative magnitude with which the downstream activation components of the cascade (i.e., C5a) are generated. Second, the kinetics of the initial complement activation via the two activation pathways by fibrillar amyloid plaques in vivo is not known, nor is it known if there is a prescribed balance between the protective vs detrimental effects due to the kinetics of activation. Third, while it is known that the classical cascade can recruit the alternative pathway and thus amplify downstream complement activation products (resulting in more robust C5a generation), it is not known to what extent this process occurs in rodent brain. In summary, the physiologic outcome may be dictated by the summation of these factors and/or others, resulting in either a net protective effect as seen in the C1q knockout model (which lacks the classical complement pathway, but has an intact alternative pathway) or a net detrimental effect as observed in the C3 knockout model (which has a complete absence of both pathways of complement activation).

In addition to the complexity of interpreting results when eliminating entire pathways of complement activation, caveats of using murine models transgenic (overexpressing) or genetically deficient in specific components or complement regulators (53) to assess their role in AD also include the potential for compensation developing in response to the lifetime of systemic complement inhibition (59), as well as the effect of the complete lack of other functions of complement system during development or injury. This has become particularly noteworthy since the early complement proteins C1q and C3 appear to play a role in normal synapse pruning (24). In light of these issues, the use of a small molecule receptor antagonist only late in the lifespan of the animal avoids those difficulties in interpreting the outcome of the modulation. The particular C5a receptor antagonist used here, PMX205, was chosen for its increased stability when administered orally (25) and for the possible higher penetration of the blood-brain barrier owing to its increased lipophilicity over PMX53, the first-generation cyclic C5aR antagonist (25–27). PMX53 has been shown to mitigate tumor progression in mice (60) and inflammatory diseases in other rodent models, including those with cerebral involvement (26, 28). When injected i.v. in rats, PMX205 was detected in brain in higher concentrations than was PMX53 (26), but the ability of PMX205 to cross the blood-brain barrier when delivered orally to mice remains to be formally determined.

While it is hypothesized that the cyclic peptide is binding to CD88 (C5aR) and thus blocking the complement activation product C5a from inducing a chemotactic and activating signal in glial cells in the brain, thereby reducing inflammation and thus neurodegeneration, note that the mechanism by which PMX205 is reducing pathology and enhancing cognition remains to be unequivocally established, particularly since C5a receptors are expressed on neurons as well (reviewed in Ref. 61). However, in contrast to other candidate C5a receptor antagonists (62), PMX205 inhibits the interaction of C5a with CD88 but not with the C5a-like receptor 2 (C5L2) (8, 62), an alternative receptor for C5a whose function is yet to be unambiguously defined (63, 64), suggesting that the beneficial effects reflect the specific inhibition of CD88. Furthermore, in an in vitro screen of 44 different receptors, PMX53 was shown to exert inhibition with only four other receptors and only at a minimum 3-fold higher concentration than that which inhibits CD88/C5aR (65). PMX205 has not yet been tested as extensively. However, it is unlikely that the effects seen here are due to nonspecific suppression of proinflammatory responses, as others have shown that PMX53 had no effect on neutrophil influx, clinical disease, or pathology in a model of experimental autoimmune encephalomyelitis (66). Additionally, treatment with PMX205 had no effect on dampening leukocyte migration to the CNS in response to intracranial inoculation with a neurotropic coronavirus (T. E. Lane, unpublished observation). Considering the weight of evidence implicating the complement system in the pathology of this AD model (reviewed in Ref. 40), the synergizing proinflammatory effects of C5a with other proinflammatory receptors such as TLR and P2Y (42, 43), the lack of observable toxicity in multiple acute rodent models previously investigated and the extended treatment in these studies, and the disease-modifying effects of PMX205 on both neuropathology and behavioral deficits presented herein, it is a compelling hypothesis that the C5a-C5aR interaction is a significant pathogenic driver in this model of AD that is mitigated by this small molecule antagonist. Future experiments are planned to further test this hypothesis.

Specific complement component-directed treatment was initiated in this study at an age at which cognitive deficits and the accumulation of fibrillar amyloid plaques have been reported by many laboratories (19, 29, 51, 67). The positive results of PMX205 treatment at this time suggest the possibility that such treatment could be effective even if started at the first recognition of cognitive decline in humans. As elaborated above, the specific inhibition of this C5a-C5aR interaction by PMX205 would allow for other demonstrated and hypothesized protective effects of complement components, including clearing apoptotic neurons and neuronal blebs, synapse pruning (during regeneration), limiting proinflammatory cytokine production, enhancing neurotrophin production (57, 58), and recruiting stem cells into the area of damage via C3a (55, 68). PMX205 has an added advantage over a Food and Drug Administration-approved anti-C5 mAb (69) or the C5-specific inhibitor from the soft tick (70) (in addition to its smaller molecular size) in that both of the latter prevent cleavage of C5 (thereby preventing C5a and C5b-9 generation), while PMX205 permits the generation of bacteriolytic C5b-9 during infection. Thus, while the recruitment of leukocytes into the area of an infection would be dampened with systemic PMX205 administration, the ability to locally generate pathogen-targeted membranolytic C5b-9 and to opsonize invading microbes with C3b (for ingestion and killing by phagocytes), as well as the presence of Ab and T cell mechanisms of immune protection,

would remain intact to provide protection from infection over even long-term treatment. Furthermore, the innate system includes redundancy, and thus other mechanisms including multiple chemokines would be functional in recruiting protective phagocytes in response to infection. Indeed, the monoclonal anti-C5 that prevents C5 cleavage has been Food and Drug Administration approved for treatment of paroxysmal nocturnal hemoglobinuria (69), and the PMX205 parent compound PMX53 has successfully passed phase I clinical trials, indicating potential safety in humans (71, 72).

In summary, the data reported herein support the hypothesis that the inhibition of C5a-induced inflammation via its receptor, CD88, reduces amyloid and tangle accumulation, reduces synapse loss, and rescues a hippocampal-dependent memory task. The observations are intriguing, and this kind of therapeutic approach is attractive due to the specificity of the pathways being inhibited, the potential for oral delivery, the lack of detrimental effects of the compound seen in multiple animal studies thus far (including long-term administration in this study), the successful phase 1 testing of PMX53 in humans, and the prediction that a PMX205-based drug could be prescribed with benefit after clinical diagnosis of early stage AD. Thus, these findings provide rationale for further investigation of the potential use of a C5a receptor antagonist as a therapeutic for AD in humans.

Acknowledgments

The authors thank Todd Metzger, Jun Zhou, Jennifer Chen, and Linda Brizuela for technical help, and Dr. M. Necula for assistance with the fibrillization assays, Dr. C. Glabe (University of California, Irvine, CA) for amyloid peptide, Drs. D. H. Cribbs, K. N. Green, and V. Vasilevko (University of California, Irvine, CA), and Dr. W. Van Nostrand (State University of New York, Stony Brook, NY) for anti-amyloid Abs and advice on the amyloid peptide ELISAs. We thank Promics for supplying C5aR antagonist for some of the initial studies.

References

1. Terry, RD.; Masliah, E.; Hansen, LA. The neuropathology of Alzheimer disease and the structural basis of its cognitive alteration. In: Terry, RD.; Katzman, R.; Bick, KL.; Sisodia, SS., editors. Alzheimer Disease. 2. Lippincott Williams & Wilkins; New York: 1999. p. 187-206.
2. Trojanowski JQ V, Lee M. Pathological tau: a loss of normal function or a gain in toxicity? Nat Neurosci. 2005; 8:1136–1137. [PubMed: 16127446]
3. Gandy S. The role of cerebral amyloid β accumulation in common forms of Alzheimer disease. J Clin Invest. 2005; 115:1121–1129. [PubMed: 15864339]
4. Wyss-Coray T. Inflammation in Alzheimer disease: driving force, bystander or beneficial response? Nat Med. 2006; 12:1005–1015. [PubMed: 16960575]
5. Shaftel SS, Griffin WS, O'Banion MK. The role of interleukin-1 in neuroinflammation and Alzheimer disease: an evolving perspective. J Neuroinflammation. 2008; 5:7. [PubMed: 18302763]
6. Aizenstein HJ, Nebes RD, Saxton JA, Price JC, Mathis CA, Tsopelas ND, Ziolko SK, James JA, Snitz BE, Houck PR, et al. Frequent amyloid deposition without significant cognitive impairment among the elderly. Arch Neurol. 2008; 65:1509–1517. [PubMed: 19001171]
7. Walport MJ. Complement: second of two parts. N Engl J Med. 2001; 344:1140–1144. [PubMed: 11297706]
8. Monk PN, Scola AM, Madala P, Fairlie DP. Function, structure and therapeutic potential of complement C5a receptors. Br J Pharmacol. 2007; 152:429– 448. [PubMed: 17603557]
9. Bonifati DM, Kishore U. Role of complement in neurodegeneration and neuroinflammation. Mol Immunol. 2007; 44:999–1010. [PubMed: 16698083]

10. Rogers J, Cooper NR, Webster S, Schultz J, McGeer PL, Styren SD, Civin WH, Brachova L, Bradt B, Ward P, Lieberburg I. Complement activation by β-amyloid in Alzheimer disease. Proc Natl Acad Sci USA. 1992; 89:10016–10020. [PubMed: 1438191]
11. Bradt BM, Kolb WP, Cooper NR. Complement-dependent proinflammatory properties of the Alzheimer's disease β-peptide. J Exp Med. 1998; 188:431– 438. [PubMed: 9687521]
12. Akiyama H, Barger S, Barnum S, Bradt B, Bauer J, Cole GM, Cooper NR, Eikelenboom P, Emmerling M, Fiebich BL, et al. Inflammation and Alzheimer's disease. Neurobiol Aging. 2000; 21:383–421. [PubMed: 10858586]
13. Loeffler DA, Camp DM, Bennett DA. Plaque complement activation and cognitive loss in Alzheimer's disease. J Neuroinflammation. 2008; 5:9. [PubMed: 18334032]
14. Zanjani H, Finch CE, Kemper C, Atkinson J, McKeel D, Morris JC, Price JL. Complement activation in very early Alzheimer disease. Alzheimer Dis Assoc Disord. 2005; 19:55– 66. [PubMed: 15942322]
15. Webster S, Lue LF, Brachova L, Tenner AJ, McGeer PL, Terai K, Walker DG, Bradt B, Cooper NR, Rogers J. Molecular and cellular characterization of the membrane attack complex, C5b-9, in Alzheimer's disease. Neurobiol Aging. 1997; 18:415– 421. [PubMed: 9330973]
16. Shen Y, Lue L, Yang L, Roher A, Kuo Y, Strohmeyer R, Goux WJ, Lee V, Johnson GV, Webster SD, et al. Complement activation by neurofibrillary tangles in Alzheimer's disease. Neurosci Lett. 2001; 305:165–168. [PubMed: 11403931]
17. Meyer-Luehmann M, Spires-Jones TL, Prada C, Garcia-Alloza M, de Calignon A, Rozkalne A, Koenigsknecht-Talboo J, Holtzman DM, Bacskai BJ, Hyman BT. Rapid appearance and local toxicity of amyloid-β plaques in a mouse model of Alzheimer's disease. Nature. 2008; 451:720–724. [PubMed: 18256671]
18. Busche MA, Eichhoff G, Adelsberger H, Abramowski D, Wiederhold KH, Haass C, Staufenbiel M, Konnerth A, Garaschuk O. Clusters of hyperactive neurons near amyloid plaques in a mouse model of Alzheimer's disease. Science. 2008; 321:1686–1689. [PubMed: 18802001]
19. Fonseca MI, Zhou J, Botto M, Tenner AJ. Absence of C1q leads to less neuropathology in transgenic mouse models of Alzheimer's disease. J Neurosci. 2004; 24:6457– 6465. [PubMed: 15269255]
20. Fan R, DeFilippis K, Van Nostrand WE. Induction of complement proteins in a mouse model for cerebral microvascular A β deposition. J Neuroinflammation. 2007; 4:22. [PubMed: 17877807]
21. Zhou J, Fonseca MI, Pisalyaput K, Tenner AJ. Complement C3 and C4 expression in C1q sufficient and deficient mouse models of Alzheimer's disease. J Neurochem. 2008; 106:2080–2092. [PubMed: 18624920]
22. Maier M, Peng Y, Jiang L, Seabrook TJ, Carroll MC, Lemere CA. Complement C3 deficiency leads to accelerated amyloid β plaque deposition and neurodegeneration and modulation of the microglia/macrophage phenotype in amyloid precursor protein transgenic mice. J Neurosci. 2008; 28:6333– 6341. [PubMed: 18562603]
23. Pisalyaput K, Tenner AJ. Complement component C1q inhibits β-amyloid- and serum amyloid P-induced neurotoxicity via caspase- and calpain-independent mechanisms. J Neurochem. 2008; 104:696–707. [PubMed: 17986223]
24. Stevens B, Allen NJ, Vazquez LE, Howell GR, Christopherson KS, Nouri N, Micheva KD, Mehalow AK, Huberman AD, Stafford B, et al. The classical complement cascade mediates CNS synapse elimination. Cell. 2007; 131:1164–1178. [PubMed: 18083105]
25. Woodruff TM, Pollitt S, Proctor LM, Stocks SZ, Manthey HD, Williams HM, Mahadevan IB, Shiels IA, Taylor SM. Increased potency of a novel complement factor 5a receptor antagonist in a rat model of inflammatory bowel disease. J Pharmacol Exp Ther. 2005; 314:811– 817. [PubMed: 15879003]
26. Woodruff TM, Crane JW, Proctor LM, Buller KM, Shek AB, de Vos K, Pollitt S, Williams HM, Shiels IA, Monk PN, Taylor SM. Therapeutic activity of C5a receptor antagonists in a rat model of neurodegeneration. FASEB J. 2006; 20:1407–1417. [PubMed: 16816116]
27. Woodruff TM, Costantini KJ, Crane JW, Atkin JD, Monk PN, Taylor SM, Noakes PG. The complement factor C5a contributes to pathology in a rat model of amyotrophic lateral sclerosis. J Immunol. 2008; 181:8727– 8734. [PubMed: 19050293]

28. Sewell DL, Nacewicz B, Liu F, Macvilay S, Erdei A, Lambris JD, Sandor M, Fabry Z. Complement C3 and C5 play critical roles in traumatic brain cryoinjury: blocking effects on neutrophil extravasation by C5a receptor antagonist. J Neuroimmunol. 2004; 155:55– 63. [PubMed: 15342196]
29. Hsiao KK, Chapman P, Nilsen S, Eckman C, Harigaya Y, Younkin S, Yang F, Cole G. Correlative memory deficits, Aβ elevations, and amyloid plaques in transgenic mice. Science. 1996; 274:99–102. [PubMed: 8810256]
30. Oddo S, Caccamo A, Shepherd JD, Murphy MP, Golde TE, Kayed R, Metherate R, Mattson MP, Akbari Y, LaFerla FM. Triple-transgenic model of Alzheimer's disease with plaques and tangles: intracellular Aβ and synaptic dysfunction. Neuron. 2003; 39:409– 421. [PubMed: 12895417]
31. Reid RC, Abbenante G, Taylor SM, Fairlie DP. A convergent solution-phase synthesis of the macrocycle Ac-Phe-[Orn-Pro-D-Cha-Trp-Arg], a potent new antiinflammatory drug. J Org Chem. 2003; 68:4464– 4471. [PubMed: 12762752]
32. Necula M, Kayed R, Milton S, Glabe CG. Small molecule inhibitors of aggregation indicate that amyloid β oligomerization and fibrillization pathways are independent and distinct. J Biol Chem. 2007; 282:10311–10324. [PubMed: 17284452]
33. Hirata-Fukae C, Li HF, Hoe HS, Gray AJ, Minami SS, Hamada K, Niikura T, Hua F, Tsukagoshi-Nagai H, Horikoshi-Sakuraba Y, et al. Females exhibit more extensive amyloid, but not tau, pathology in an Alzheimer transgenic model. Brain Res. 2008; 1216:92–103. [PubMed: 18486110]
34. Decker MW, Gill TM, McGaugh JL. Concurrent muscarinic and β-adrenergic blockade in rats impairs place-learning in a water maze and retention of inhibitory avoidance. Brain Res. 1990; 513:81– 85. [PubMed: 2161697]
35. King DL, Arendash GW. Behavioral characterization of the Tg2576 transgenic model of Alzheimer's disease through 19 months. Physiol Behav. 2002; 75:627– 642. [PubMed: 12020728]
36. Nolte C, Möller T, Walter T, Kettenmann H. Complement 5a controls motility of murine microglial cells in vitro via activation of an inhibitory G-protein and the rearrangement of the actin cytoskeleton. Neuroscience. 1996; 73:1091–1107. [PubMed: 8809827]
37. Tenner, AJ.; Pisalyaput, K. The complement system in the CNS: thinking again. In: Lane, TE.; Carson, MJ.; Bergmann, C.; Wyss-Coray, T., editors. Central Nervous System Diseases and Inflammation. Springer; New York: 2008. p. 153-174.
38. Afagh A, Cummings BJ, Cribbs DH, Cotman CW, Tenner AJ. Localization and cell association of C1q in Alzheimer's disease brain. Exp Neurol. 1996; 138:22–32. [PubMed: 8593893]
39. Yao J, Harvath L, Gilbert DL, Colton CA. Chemotaxis by a CNS macrophage, the microglia. J Neurosci Res. 1990; 27:36– 42. [PubMed: 2254955]
40. Alexander JJ, Anderson AJ, Barnum SR, Stevens B, Tenner AJ. The complement cascade: Yin-Yang in neuroinflammation: neuroprotection and -degeneration. J Neurochem. 2008; 107:1169–1187. [PubMed: 18786171]
41. Rojo LE, Fernandez JA, Maccioni AA, Jimenez JM, Maccioni RB. Neuroinflammation: implications for the pathogenesis and molecular diagnosis of Alzheimer's disease. Arch Med Res. 2008; 39:1–16. [PubMed: 18067990]
42. Flaherty P, Radhakrishnan ML, Dinh T, Rebres RA, Roach TI, Jordan MI, Arkin AP. A dual receptor crosstalk model of G-protein-coupled signal transduction. PLoS Comput Biol. 2008; 4:e1000185. [PubMed: 18818727]
43. Zhang X, Kimura Y, Fang C, Zhou L, Sfyroera G, Lambris JD, Wetsel RA, Miwa T, Song WC. Regulation of Toll-like receptor-mediated inflammatory response by complement in vivo. Blood. 2007; 110:228–236. [PubMed: 17363730]
44. Hawlisch H, Belkaid Y, Baelder R, Hildeman D, Gerard C, Kohl J. C5a negatively regulates Toll-like receptor 4-induced immune responses. Immunity. 2005; 22:415– 426. [PubMed: 15845447]
45. Patel SN, Berghout J, Lovegrove FE, Ayi K, Conroy A, Serghides L, Minoo G, Gowda DC, Sarma JV, Rittirsch D, et al. C5 deficiency and C5a or C5aR blockade protects against cerebral malaria. J Exp Med. 2008; 205:1133–1143. [PubMed: 18426986]
46. Tahara K, Kim HD, Jin JJ, Maxwell JA, Li L, Fukuchi K. Role of Toll-like receptor signalling in Aβ uptake and clearance. Brain. 2006; 129:3006–3019. [PubMed: 16984903]

47. Jana M, Palencia CA, Pahan K. Fibrillar amyloid-β peptides activate microglia via TLR2: implications for Alzheimer's disease. J Immunol. 2008; 181:7254–7262. [PubMed: 18981147]
48. Lim GP, Yang F, Chu T, Chen P, Beech W, Teter B, Tran T, Ubeda O, Ashe KH, Frautschy SA, Cole GM. Ibuprofen suppresses plaque pathology and inflammation in a mouse model for Alzheimer's disease. J Neurosci. 2000; 20:5709–5714. [PubMed: 10908610]
49. Ryman D, Gao Y, Lamb BT. Genetic loci modulating amyloid-β levels in a mouse model of Alzheimer's disease. Neurobiol Aging. 2008; 29:1190–1198. [PubMed: 17400334]
50. Jain NK, Patil CS, Kulkarni SK, Singh A. Modulatory role of cyclooxygenase inhibitors in aging- and scopolamine or lipopolysaccharide-induced cognitive dysfunction in mice. Behav Brain Res. 2002; 133:369–376. [PubMed: 12110471]
51. Ognibene E, Middei S, Daniele S, Adriani W, Ghirardi O, Caprioli A, Laviola G. Aspects of spatial memory and behavioral disinhibition in Tg2576 transgenic mice as a model of Alzheimer's disease. Behav Brain Res. 2005; 156:225–232. [PubMed: 15582108]
52. Bergamaschini L, Rossi E, Storini C, Pizzimenti S, Distaso M, Perego C, De Luigi A, Vergani C, Grazia DS. Peripheral treatment with enoxaparin, a low molecular weight heparin, reduces plaques and β-amyloid accumulation in a mouse model of Alzheimer's disease. J Neurosci. 2004; 24:4181– 4186. [PubMed: 15115813]
53. Wyss-Coray T, Yan F, Lin AH, Lambris JD, Alexander JJ, Quigg RJ, Masliah E. Prominent neurodegeneration and increased plaque formation in complement-inhibited Alzheimer's mice. Proc Natl Acad Sci USA. 2002; 99:10837–10842. [PubMed: 12119423]
54. Pasinetti GM, Tocco G, Sakhi S, Musleh WD, DeSimoni MG, Mascarucci P, Schreiber S, Baudry M, Finch CE. Hereditary deficiencies in complement C5 are associated with intensified neurodegenerative responses that implicate new roles for the C-system in neuronal and astrocytic functions. Neurobiol Dis. 1996; 3:197–204. [PubMed: 8980020]
55. Rahpeymai Y, Hietala MA, Wilhelmsson U, Fotheringham A, Davies I, Nilsson AK, Zwirner J, Wetsel RA, Gerard C, Pekny M, Pekna M. Complement: a novel factor in basal and ischemia-induced neurogenesis. EMBO J. 2006; 25:1364–1374. [PubMed: 16498410]
56. Rus H, Cudrici C, Niculescu F. C5b-9 complement complex in autoimmune demyelination and multiple sclerosis: dual role in neuroinflammation and neuroprotection. Ann Med. 2005; 37:97–104. [PubMed: 16026117]
57. Jauneau AC, Ischenko A, Chatagner A, Benard M, Chan P, Schouft MT, Patte C, Vaudry H, Fontaine M. Interleukin 1b and anaphylatoxins exert a synergistic effect on NGF expression by astrocytes. J Neuroinflammation. 2006; 3:8. [PubMed: 16594997]
58. Heese K, Hock C, Otten U. Inflammatory signals induce neurotrophin expression in human microglial cells. J Neurochem. 1998; 70:699–707. [PubMed: 9453564]
59. Kang HJ, Bao L, Xu Y, Quigg RJ, Giclas PC, Holers VM. Increased serum C3 levels in Crry transgenic mice partially abrogates its complement inhibitory effects. Clin Exp Immunol. 2004; 136:194–199. [PubMed: 15086380]
60. Markiewski MM, DeAngelis RA, Benencia F, Ricklin-Lichtsteiner SK, Koutoulaki A, Gerard C, Coukos G, Lambris JD. Modulation of the antitumor immune response by complement. Nat Immunol. 2008; 9:1225–1235. [PubMed: 18820683]
61. Nataf S, Stahel PF, Davoust N, Barnum SR. Complement anaphylatoxin receptors on neurons: new tricks for old receptors? Trends Neurosci. 1999; 22:397– 402. [PubMed: 10441300]
62. Otto M, Hawlisch H, Monk PN, Muller M, Klos A, Karp CL, Kohl J. C5a mutants are potent antagonists of the C5a receptor (CD88) and of C5L2: position 69 is the locus that determines agonism or antagonism. J Biol Chem. 2004; 279:142–151. [PubMed: 14570896]
63. Gavrilyuk V, Kalinin S, Hilbush BS, Middlecamp A, McGuire S, Pelligrino D, Weinberg G, Feinstein DL. Identification of complement 5a-like receptor (C5L2) from astrocytes: characterization of anti-inflammatory properties. J Neurochem. 2005; 92:1140–1149. [PubMed: 15715664]
64. Rittirsch D, Flierl MA, Nadeau BA, Day DE, Huber-Lang M, Mackay CR, Zetoune FS, Gerard NP, Cianflone K, Kohl J, et al. Functional roles for C5a receptors in sepsis. Nat Med. 2008; 14:551–557. [PubMed: 18454156]

65. Schnatbaum K, Locardi E, Scharn D, Richter U, Hawlisch H, Knolle J, Polakowski T. Peptidomimetic C5a receptor antagonists with hydrophobic substitutions at the C-terminus: increased receptor specificity and in vivo activity. Bioorg Med Chem Lett. 2006; 16:5088–5092. [PubMed: 16876401]

66. Morgan BP, Griffiths M, Khanom H, Taylor SM, Neal JW. Blockade of the C5a receptor fails to protect against experimental autoimmune encephalomyelitis in rats. Clin Exp Immunol. 2004; 138:430– 438. [PubMed: 15544619]

67. Frautschy SA, Yang FS, Irrizarry M, Hyman B, Saido TC, Hsiao K, Cole GM. Microglial response to amyloid plaques in APPsw transgenic mice. Am J Pathol. 1998; 152:307–317. [PubMed: 9422548]

68. Bogestal YR, Barnum SR, Smith PL, Mattisson V, Pekny M, Pekna M. Signaling through C5aR is not involved in basal neurogenesis. J Neurosci Res. 2007; 85:2892–2897. [PubMed: 17551982]

69. Rother RP, Rollins SA, Mojcik CF, Brodsky RA, Bell L. Discovery and development of the complement inhibitor eculizumab for the treatment of paroxysmal nocturnal hemoglobinuria. Nat Biotech. 2007; 25:1256–1264.

70. Hepburn NJ, Williams AS, Nunn MA, Chamberlain-Banoub JC, Hamer J, Morgan BP, Harris CL. In vivo characterization and therapeutic efficacy of a C5-specific inhibitor from the soft tick *Ornithodoros moubata*. J Biol Chem. 2007; 282:8292– 8299. [PubMed: 17215252]

71. Woodruff TM, Proctor LM, Strachan AJ, Taylor SM. Complement factor 5a as a therapeutic target. Drugs Future. 2006; 31:325–334.

72. Kohl J. Drug evaluation: the C5a receptor antagonist PMX-53. Curr Opin Mol Ther. 2006; 8:529–538. [PubMed: 17243489]

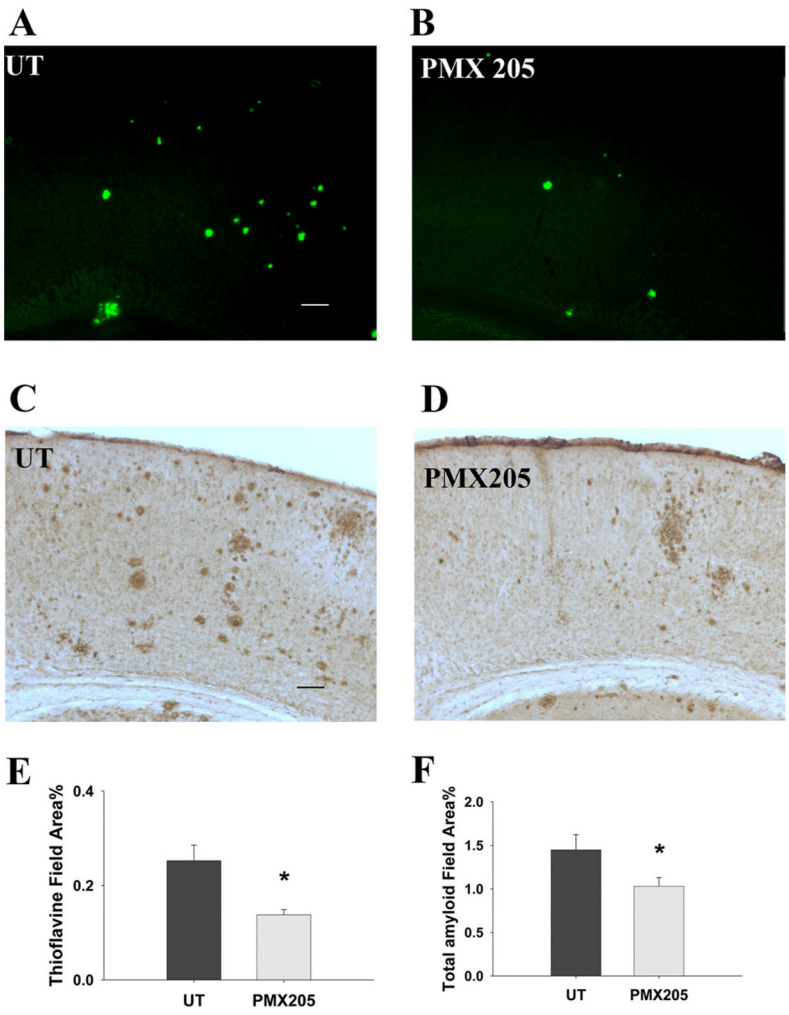

FIGURE 1.

Treatment with PMX205 decreases fibrillar and total amyloid. Representative images of fibrillar (thioflavine staining) amyloid (*A* and *B*) and total (6E10 staining) amyloid (*C* and *D*) in cortex of Tg2576 mice treated without (*A* and *C*) or with 20 μg/ml PMX205 (*B* and *D*) in the drinking water for 12 wk (from age 12 to15 mo). Scale bar, 100 μm. *E* and *F*, Quantification of thioflavine (*E*) or 6E10 (*F*) staining in cortex and hippocampus by image analysis shows significant decreases in fibrillar amyloid (44%, $p < 0.0006$) and total amyloid (29%, $p < 0.03$) in treated animals. Bars represent the group means ± SEM of *n* animals per condition (UT, $n = 11$; PMX205, $n = 17$).

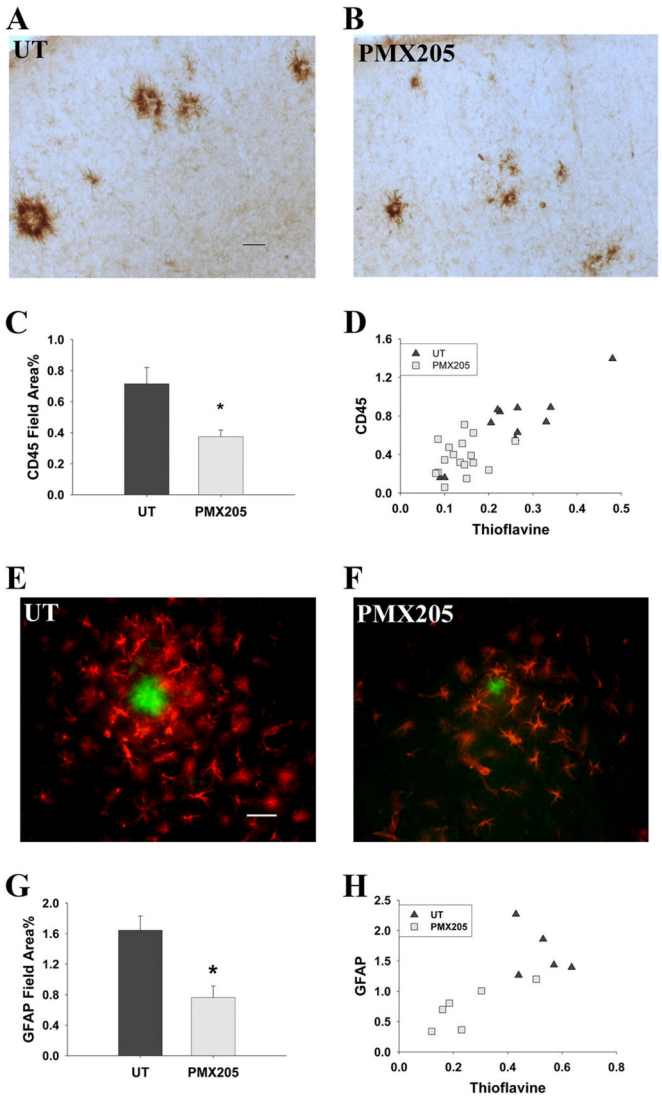

FIGURE 2.

PMX205 treatment significantly reduces reactive microglia and astrocytes. CD45 (*A* and *B*) and GFAP (red)/thioflavine (green) (*E* and *F*) staining in the cortex of untreated (*A* and *E*) and PMX205-treated (*B* and *F*) Tg2576 mice. Scale bar, 50 μm. Image analysis indicates that PMX205 treatment caused a significant decrease of activated microglia (*C*) (49%, $p < 0.002$) and reactive astrocytes (*G*) in the proximity of the plaques (54%, $p < 0.003$). Bars represent the group means ± SEM from *n* animals per condition (UT, $n = 11$ and PMX205, $n = 17$ for CD45; UT, $n = 5$ and PMX205, $n = 6$ for GFAP). Correlation of thioflavine and CD45 (*D*) or GFAP (*H*) staining in individual animals ($R = 0.82$, $p < 0.0001$; $R = 0.74$, $p < 0.01$, respectively). Squares represent PMX205-treated animals; triangles represent untreated animals.

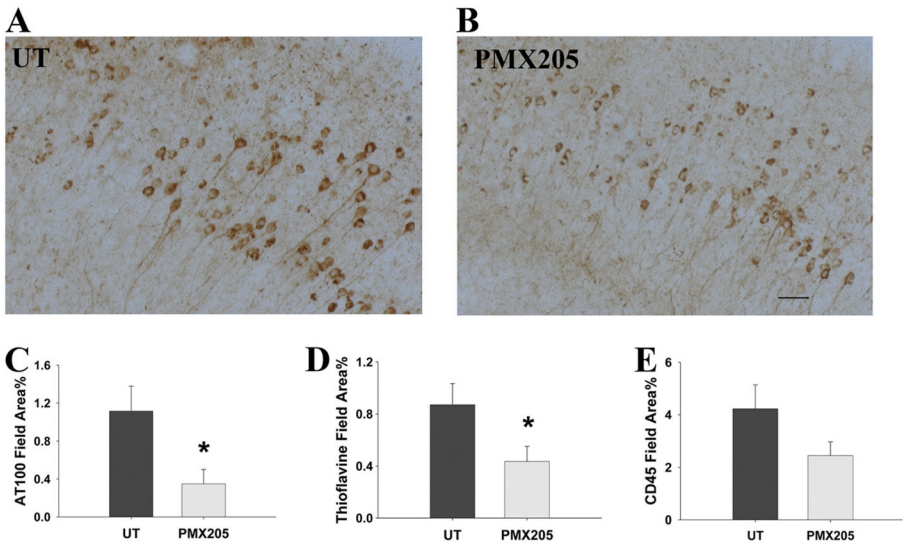

FIGURE 3.

PMX205 treatment decreases hyperphosphorylated tau in 3xTg mice. Representative images of AT100 (phosphorylated Ser^{212} and Thr^{214} tau) staining of the subiculum area of hippocampus in female 3xTg mice that were treated with 20 μg/ml PMX205 in the drinking water (*B*) or untreated (*A*) for 12 wk (from 17 to 20 mo). Scale bar, 50 μm. *C*, Image analysis of AT100 shows significantly lower immunoreactivity (69%, $p < 0.02$) in antagonist-treated animals. Quantification of thioflavine (*D*) and CD45 (*E*) staining show a significant reduction in thioflavine (49%, $p < 0.05$) and a trend for decrease in CD45 (42%, $p < 0.12$) in PMX205-treated animals. Bars represent the group mean ± SEM of *n* animals (pooled from two independent trials) per condition (UT, $n = 9$; PMX, $n = 9$).

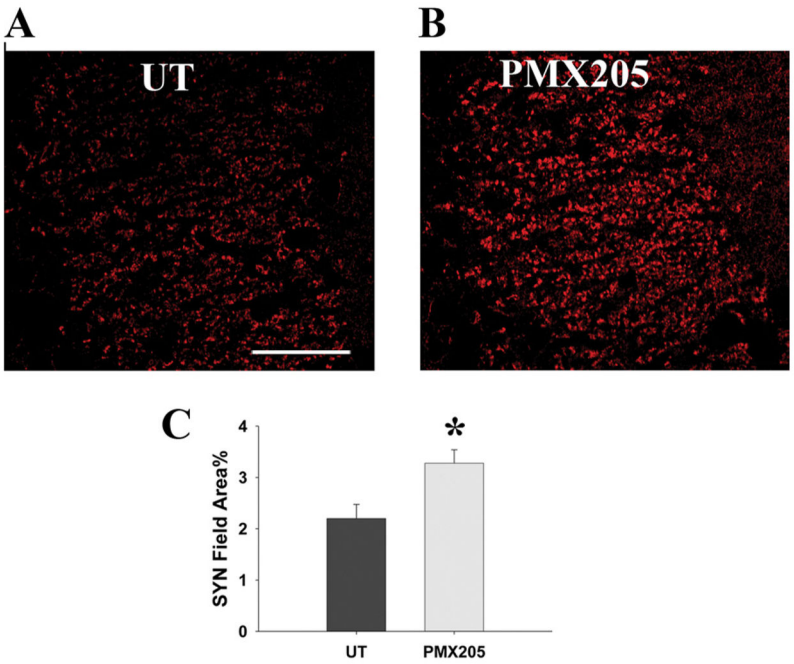

FIGURE 4.

SYN immunoreactivity is higher in PMX205-treated Tg2576. Confocal fluorescent microscopy of SYN immunostaining in the CA3a area of hippocampus of untreated (*A*) or PMX205-treated (*B*) Tg2576 mice. *C*, Quantification of SYN immunostaining in CA3a and CA3c areas of hippocampus indicates that there is a 33% ($p < 0.03$) increase in immunolabelled area. Data are expressed as mean values ± SEM of *n* animals per condition (UT, $n = 4$; PMX205, $n = 7$). Scale bar, 50 um.

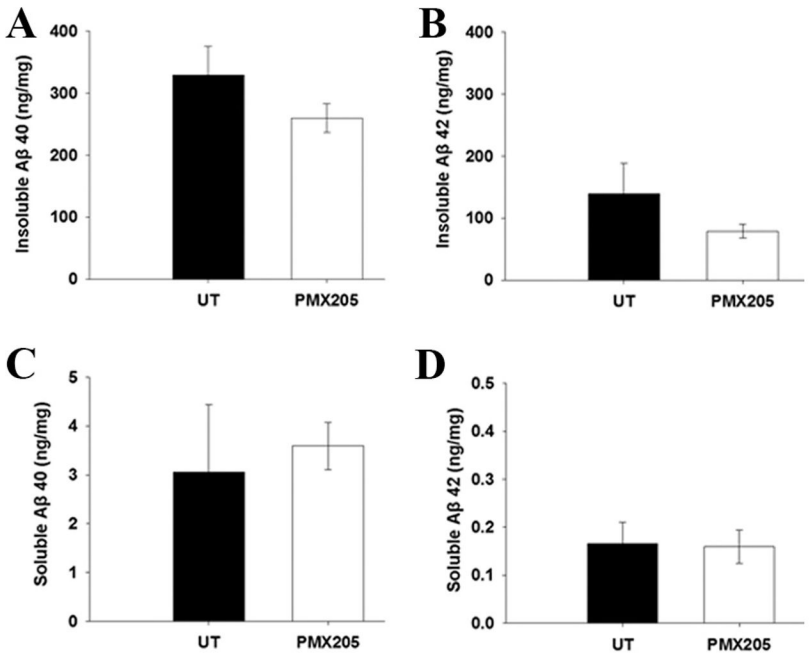

FIGURE 5.

Treatment with PMX205 reduces T-PER-insoluble amyloid. Cortices from PMX205-treated and untreated Tg2576 mice were extracted first with T-PER buffer (*C* and *D*) and then the insoluble pellet extracted with formic acid (*A* and *B*). Each fraction was analyzed for Aβ_{40} and Aβ_{42} and expressed as nanograms per milligram total brain protein. In the detergent-insoluble, formic acid fraction, Aβ_{40} and Aβ_{42} were reduced 21% and 43%, respectively, by drug treatment ($p = 0.198$ and $p = 0.272$, respectively, calculated using an unpaired Student's *t* test after performing log transformation to account for group variance). Error bars represent the group means ± SEM of *n* animals per condition (UT, $n = 6$; PMX205, $n = 10$).

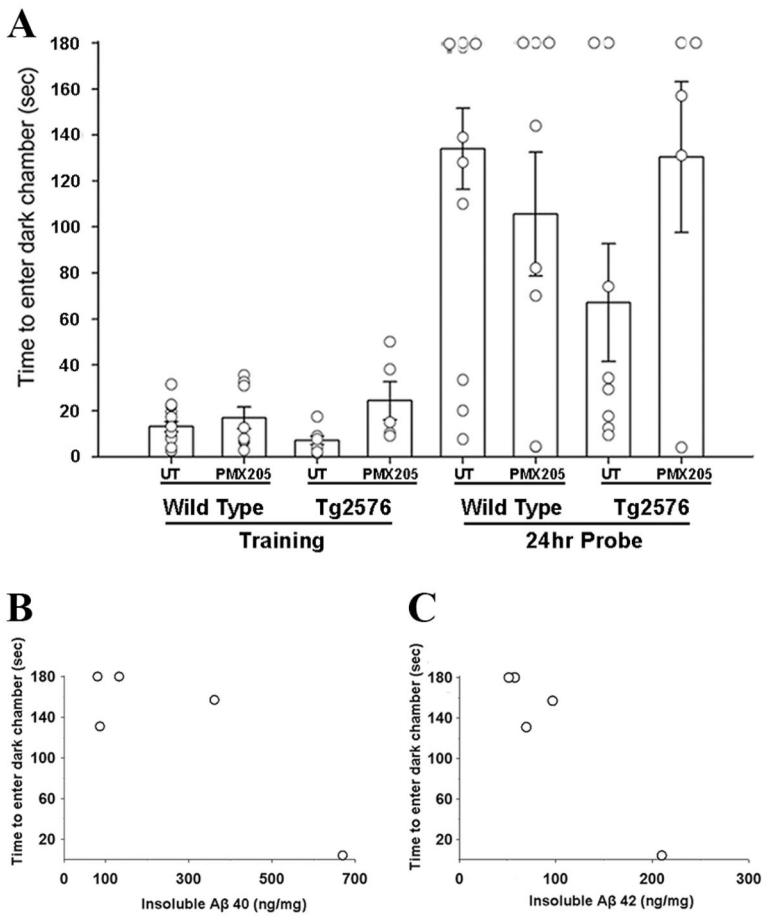

FIGURE 6.

Cognitive function is improved following PMX205 treatment. *A*, Memory retention was measured in 15-mo-old mice by their ability to recall an aversive stimulus given during passive avoidance training 24 h earlier. UT Tg2576 mice displayed a significant reduction in memory retention compared with wild-type (WT) mice (67.1 s vs 134 s, $p < 0.04$), and this deficit was rescued after PMX205 treatment (130 s). Circles represent individual animals (overlapping scores in each of the training groups and in the 24 h wild-type animals prevent visualization of all individual animals). The *p* value was determined using an unpaired Student's *t* test. Error bars represent the ± SEM of *n* animals (WT-UT, $n = 14$; WT + PMX205, $n = 8$; Tg2576-UT, $n = 8$; Tg2576 + PMX205, $n = 5$). Correlation analysis between cognitive performance and detergent-insoluble Aβ_{40} (*B*) and Aβ_{42} (*C*) levels in hippocampus of PMX205-treated mice ($n = 5$); $R = -0.87$, $p = 0.058$ and $R = -0.96$, $p < 0.01$, respectively, using Pearson product moment correlation.

Table I

Summary of pilot trials of PMX205 treatment

Trial No.	No. Animals Untreated/Treated	Age (mo)	PMX205 (μg/ml, drinking water)	PMX205 (mg/kg, s.c.)	Treatment Length (wk)	% Decrease (PMX treated from untreated)			
						Thioflavine	Total amyloid	CD45	GFAP
1a	5/3	11–14	10		12	33	34	15	5
1b	5/8	11–14	10	1	12	59***	51**	49*	40
2a	5/3	11–13	20		8	62**	69*	68**	48*
2b	5/4	11–13	20	1	8	46*	54	48*	44*

*** $p < 0.001$;

** $p < 0.01$;

* $p < 0.05$.